**Supporting information for**

# Old Donors for New Molecular Conductors: Combining TMTSF and BEDT-TTF with Anionic $(TaF_6)_{1-x}/(PF_6)_x$ Alloys

**Magali Allain [1], Cécile Mézière [1], Pascale Auban-Senzier [2] and Narcis Avarvari [1,*]**

[1] Univ Angers, CNRS, MOLTECH-Anjou, SFR MATRIX, F-49000 Angers, France; magali.allain@univ-angers.fr; cecile.meziere@univ-angers.fr

[2] Laboratoire de Physique des Solides, Université Paris-Saclay CNRS UMR 8502, Bât. 510, 91405 Orsay, France; senzier@lps.u-psud.fr

* Correspondence: narcis.avarvari@univ-angers.fr; Tel.: +33-2-4173-5084

## Single crystal X-ray crystallography

**Table S1**. Crystal Data and Structure Refinement for $(TMTSF)_2(TaF_6)_{0.12}(PF_6)_{0.88}$, $(TMTSF)_2(TaF_6)_{0.44}(PF_6)_{0.56}$, $(TMTSF)_2(TaF_6)_{0.56}(PF_6)_{0.44}$ and $(TMTSF)_2(TaF_6)_{0.84}(PF_6)_{0.16}$.

| Compound | **$(TMTSF)_2$ $(TaF_6)_{0.12}(PF_6)_{0.88}$** | **$(TMTSF)_2$ $(TaF_6)_{0.44}(PF_6)_{0.56}$** | **$(TMTSF)_2$ $(TaF_6)_{0.56}(PF_6)_{0.44}$** | **$(TMTSF)_2$ $(TaF_6)_{0.84}(PF_6)_{0.16}$** |
|---|---|---|---|---|
| Empirical formula | $C_{20}H_{24}F_6P_{0.88}Se_8Ta_{0.12}$ | $C_{20}H_{24}F_6P_{0.56}Se_8Ta_{0.44}$ | $C_{20}H_{24}F_6P_{0.44}Se_8Ta_{0.56}$ | $C_{20}H_{24}F_6P_{0.16}Se_8Ta_{0.84}$ |
| Molecular weight | 1059.49 | 1107.78 | 1125.63 | 1167.02 |
| T (K) | 296(2) | 293(2) | 293(2) | 293(2) |
| Wavelength (Å) | 1.54184 | 1.54184 | 1.54184 | 1.54184 |
| Crystal system | Triclinic | Triclinic | Triclinic | Triclinic |
| Space group | *P*-1 | *P*-1 | *P*-1 | *P*-1 |
| *a* (Å) | 7.2868(8) | 7.2916(4) | 7.2939(7) | 7.2911(8) |
| *b* (Å) | 7.708(1) | 7.7185(4) | 7.7194(6) | 7.7323(9) |
| *c* (Å) | 13.5513(8) | 13.6966(5) | 13.748(1) | 13.8709(8) |
| α(deg) | 83.285(8) | 83.021(4) | 83.080(7) | 82.821(7) |
| *β*(deg) | 86.195(6) | 85.826(4) | 85.783(8) | 85.416(7) |
| *γ*(deg) | 71.09(1) | 71.339(5) | 71.365(8) | 71.66(1) |
| *V* (Å$^3$) | 714.8(1) | 724.44(6) | 727.6(1) | 735.8(1) |
| *Z* | 1 | 1 | 1 | 1 |
| $D_c$ (g cm$^{-3}$) | 2.461 | 2.539 | 2.569 | 2.634 |
| F(000) | 492 | 511 | 518 | 534 |
| Abs coeff (mm$^{-1}$) | 13.734 | 15.534 | 16.196 | 17.691 |
| Crystal size (mm$^3$) | 0.188× 0.028 × 0.016 | 0.141× 0.032 × 0.024 | 0.13× 0.021 × 0.012 | 0.092× 0.017 × 0.016 |
| θ (min / max) | 3.285 / 73.994 | 3.253 / 75.812 | 3.240 / 76.297 | 3.214 / 72.067 |
| Transmission (min/max) | 0.934 / 1.000 | 0.285 / 0.698 | 0.642 / 1.000 | 0.973 / 1.000 |
| Data collected/unique | 5167 / 2769 | 6386 / 2954 | 5263 / 2932 | 5154 / 2811 |
| Data observed | 1968 | 2733 | 2402 | 2382 |
| *R* (int) | 0.0334 | 0.0195 | 0.0344 | 0.0312 |
| GOF on $F^2$ | 1.024 | 1.038 | 1.021 | 1.028 |
| final *R* indices[a] [$I > 2\sigma(I)$] | $R_1$ = 0.0380, $wR_2$ = 0.0889 | $R_1$ = 0.0274, $wR_2$ = 0.0705 | $R_1$ = 0.0412, $wR_2$ = 0.0988 | R1 = 0.0354, wR2 = 0.0869 |
| *R* indices (all data) | $R_1$ = 0.0597, $wR_2$ = 0.0998 | $R_1$ = 0.0297, $wR_2$ = 0.0725 | $R_1$ = 0.0522, $wR_2$ = 0.1060 | R1 = 0.0444, wR2 = 0.0929 |
| Largest peak in final: difference (e A$^{-3}$) | 0.479 / -0.751 | 0.670 / -0.722 | 0.752 / -0.935 | 0.865 / -0.659 |
| CCDC number | 2071481 | 2071482 | 2071483 | 2071484 |

[a] $R(F) = \Sigma||F_o| - |F_c||/\Sigma|F_o|$; $wR(F^2) = [\Sigma[w(F_o^2 - F_c^2)^2]/\Sigma[w(F_o^2)^2]]^{1/2}$

**Table S2**. Crystal Data and Structure Refinement for $(TMTSF)_2TaF_6$ (293 K and 100 K), $\delta_o$-$(BEDT\text{-}TTF)_2(TaF_6)_{0.43}(PF_6)_{0.57}$, $\delta_m$-$(BEDT\text{-}TTF)_2(TaF_6)_{0.94}(PF_6)_{0.06}$, and $(BEDT\text{-}TTF)_2(TaF_6)_2{\cdot}CH_2Cl_2$.

| Compound | **$(TMTSF)_2TaF_6$** | **$(TMTSF)_2TaF_6$** | **$\delta_o$-$(BEDT\text{-}TTF)_2(TaF_6)_{0.43}(PF_6)_{0.57}$** | **$\delta_m$-$(BEDT\text{-}TTF)_2(TaF_6)_{0.94}(PF_6)_{0.06}$** | **$(BEDT\text{-}TTF)_2(TaF_6)_2$, $CH_2Cl_2$** |
|---|---|---|---|---|---|
| Empirical formula | $C_{20}H_{24}F_6Se_8Ta$ | $C_{20}H_{24}F_6Se_8Ta$ | $C_{20}H_{16}F_6P_{0.57}S_{16}Ta_{0.43}$ | $C_{20}H_{16}F_6P_{0.06}S_{16}Ta_{0.94}$ | $C_{21}H_{18}Cl_2F_{12}S_{16}Ta_2$ |
| Molecular weight | 1191.02 | 1191.02 | 979.35 | 1055.54 | 1444.11 |
| T (K) | 293(2) | 100(1) | 295(2) | 298(2) | 295(2) |
| Wavelength (Å) | 1.54184 | 1.54184 | 1.54184 | 1.54184 | 1.54184 |
| Crystal system | Triclinic | Triclinic | Orthorhombic | Monoclinic | Triclinic |
| Space group | *P*-1 | *P*-1 | *Pnna* | *I*2/*a* [b] | *P*-1 |
| *a* (Å) | 7.3130(8) | 7.1344(4) | 14.9866(4) | 14.939(1) | 8.2558(2) |
| *b* (Å) | 7.7519(7) | 7.7255(5) | 33.0248(7) | 6.6793(4) | 9.8754(4) |
| *c* (Å) | 13.898(1) | 13.7204(9) | 6.6706(1) | 33.584(1) | 12.7497(5) |
| α(deg) | 82.854(7) | 83.378(5) | 90 | 90 | 80.069(4) |
| *β*(deg) | 85.340(8) | 87.118(5) | 90 | 93.914(5) | 85.341(3) |
| *γ*(deg) | 71.728(9) | 70.200(6) | 90 | 90 | 79.823(3) |
| *V* (Å$^3$) | 741.6(1) | 706.72(8) | 3301.5(1) | 3343.1(3) | 1006.41(6) |
| *Z* | 1 | 1 | 4 | 4 | 1 |
| $D_c$ (g cm$^{-3}$) | 2.667 | 2.798 | 1.970 | 2.097 | 2.383 |
| F(000) | 543 | 543 | 1945 | 2063 | 688 |
| Abs coeff (mm$^{-1}$) | 18.515 | 19.428 | 13.032 | 15.582 | 19.562 |
| Crystal size (mm$^3$) | 0.098× 0.061 × 0.022 | 0.098× 0.061 × 0.022 | 0.215× 0.149 × 0.061 | 0.118× 0.049 × 0.019 | 0.329× 0.062 × 0.031 |
| θ (min / max) | 3.208 / 73.734 | 3.243 / 73.023 | 2.676 / 76.021 | 2.638 / 71.997 | 3.524 / 76.193 |
| Transmission (min/max) | 0.444 / 1.000 | 0.536 / 1.000 | 0.440 / 1.000 | 0.310 / 0.767 | 0.090 / 0.735 |
| Data collected/unique | 4659 / 2820 | 4463 / 2680 | 10452 / 3435 | 7179 / 3214 | 7612 / 4063 |
| Data observed | 2063 | 2524 | 3187 | 2534 | 3952 |
| *R* (int) | 0.0585 | 0.0268 | 0.0191 | 0.0338 | 0.0206 |
| GOF on $F^2$ | 0.948 | 1.030 | 1.044 | 1.090 | 1.023 |
| final *R* indices[a] [$I > 2\sigma(I)$] | R1 = 0.0476, wR2 = 0.11404 | R1 = 0.0317, wR2 = 0.0843 | $R_1$ = 0.0359, $wR_2$ = 0.0854 | $R_1$ = 0.0450, $wR_2$ = 0.1098 | R1 = 0.0316, wR2 = 0.0860 |
| *R* indices (all data) | R1 = 0.0652, wR2 = 0.1271 | R1 = 0.0341, wR2 = 0.0876 | $R_1$ = 0.0386, $wR_2$ = 0.0875 | $R_1$ = 0.0593, $wR_2$ = 0.1186 | R1 = 0.0321, wR2 = 0.0866 |
| Largest peak in final: difference (e A$^{-3}$) | 1.030 / -0.852 | 1.171 / -1.617 | 0.771 / -0.783 | 1.016 / -0.538 | 1.874 / -1.436 |
| CCDC number | 2071485 | 2071486 | 2071487 | 2071488 | 2071489 |

[a] $R(F) = \Sigma||F_o| - |F_c||/\Sigma|F_o|$; $wR\ (F^2) = [\Sigma[w(F_o^2 - F_c^2)^2]/\Sigma[w(F_o^2)^2]]^{1/2}$

[b] Reduced cell in *P*-1 space group: a = 6.6738(4) Å, b = 14.947(1) Å, c = 18.213(1) Å, α = 110.307(7)°, β = 100.540(6)°, γ = 90.006(6)°, V = 1671.2(2) Å

## Crystal structures of TMTSF salts

Compound $(TMTSF)_2(TaF_6)_{0.12}(PF_6)_{0.88}$

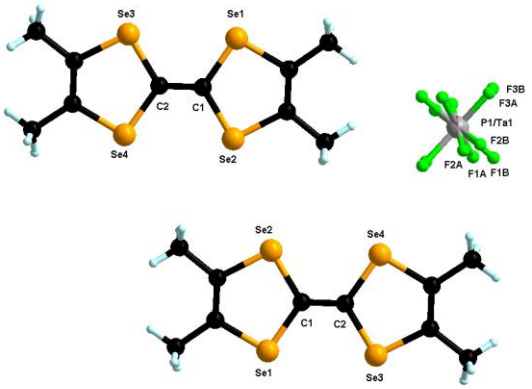


**Figure S1.** Molecular structure of $(TMTSF)_2(TaF_6)_{0.12}(PF_6)_{0.88}$. The three independent fluorine atoms of the anion are disordered over two positions with partial refined occupancy factors of 0.78/0.22.

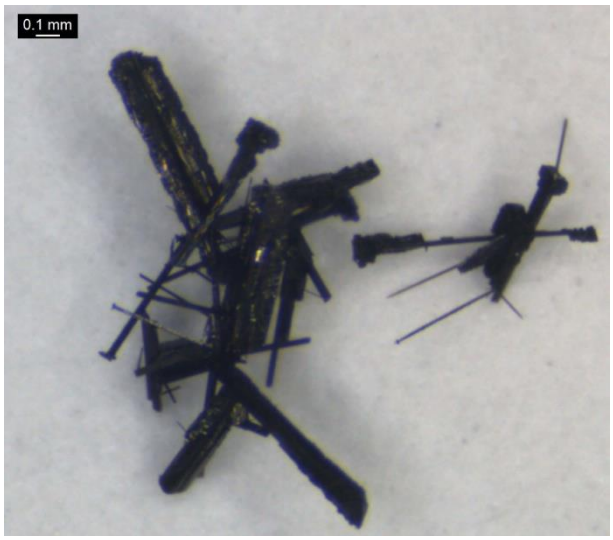


**Figure S2.** Picture of $(TMTSF)_2(TaF_6)_{0.12}(PF_6)_{0.88}$ needles with nested black platelets of $(TMTSF)_3Ta_2F_{10}O$.

Compounds $(TMTSF)_2(TaF_6)_{0.44}(PF_6)_{0.56}$

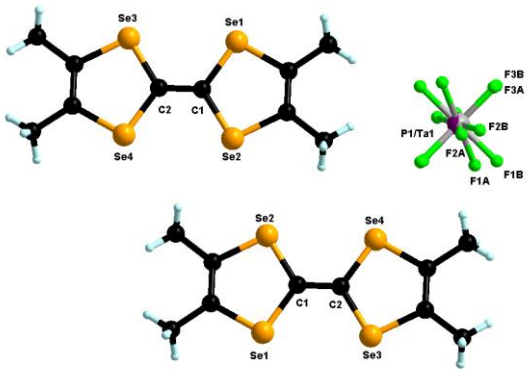


**Figure S3.** Molecular structure of $(TMTSF)_2(TaF_6)_{0.44}(PF_6)_{0.56}$. The three independent fluoride atoms of the anion are disordered over two positions with partial refined occupancy factors of 0.76/0.24.

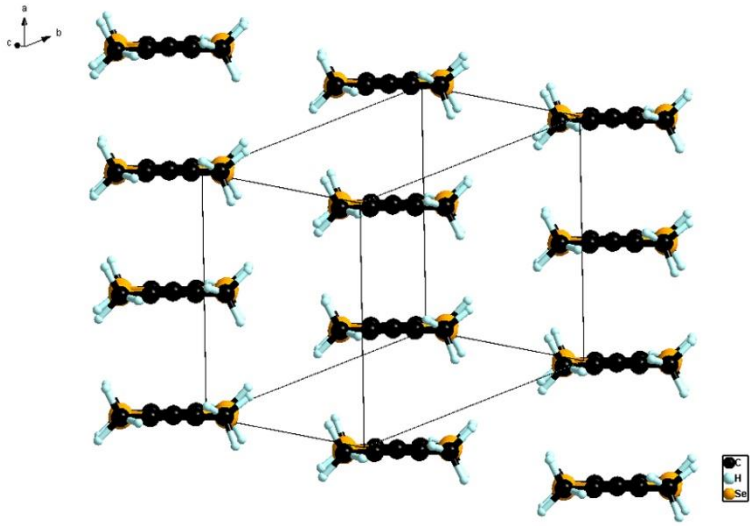


**Figure S4.** Packing of donors in the structure of $(TMTSF)_2(TaF_6)_{0.44}(PF_6)_{0.56}$.

Compounds $(TMTSF)_2(TaF_6)_{0.56}(PF_6)_{0.44}$

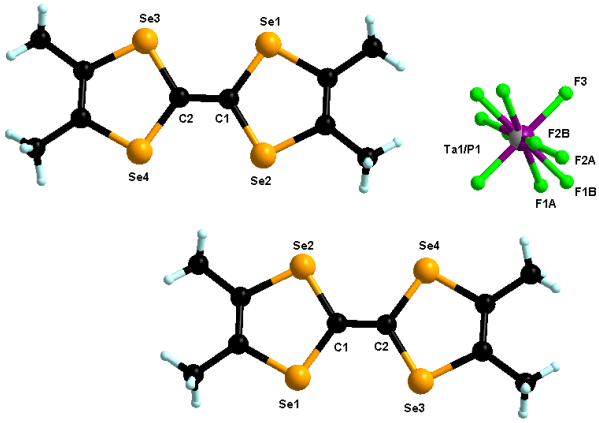


**Figure S5.** Molecular structure of $(TMTSF)_2(TaF_6)_{0.56}(PF_6)_{0.44}$. Two of the three independent fluoride atoms of the anion are disordered over two positions with partial refined occupancy factors of 0.71/0.29.

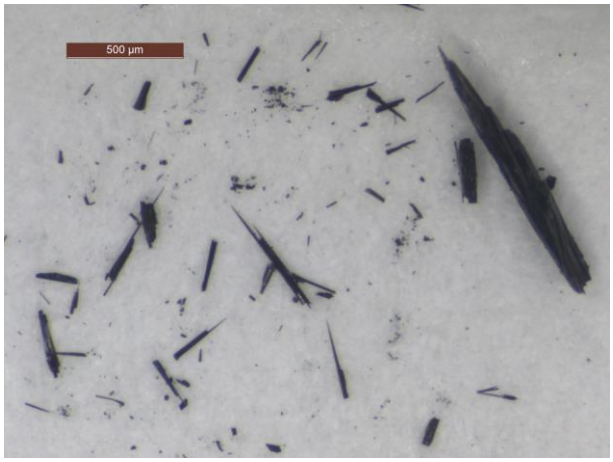


**Figure S6.** Picture of $(TMTSF)_2(TaF_6)_{0.56}(PF_6)_{0.44}$ thin needles.

Compound $(TMTSF)_2(TaF_6)_{0.84}(PF_6)_{0.16}$

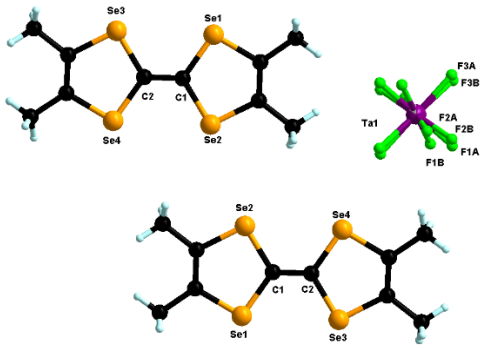


**Figure S7.** Molecular structure of $(TMTSF)_2(TaF_6)_{0.84}(PF_6)_{0.16}$. The three independent fluoride atoms of the anion are disordered over two positions with partial refined occupancy factors of 0.61/0.39.

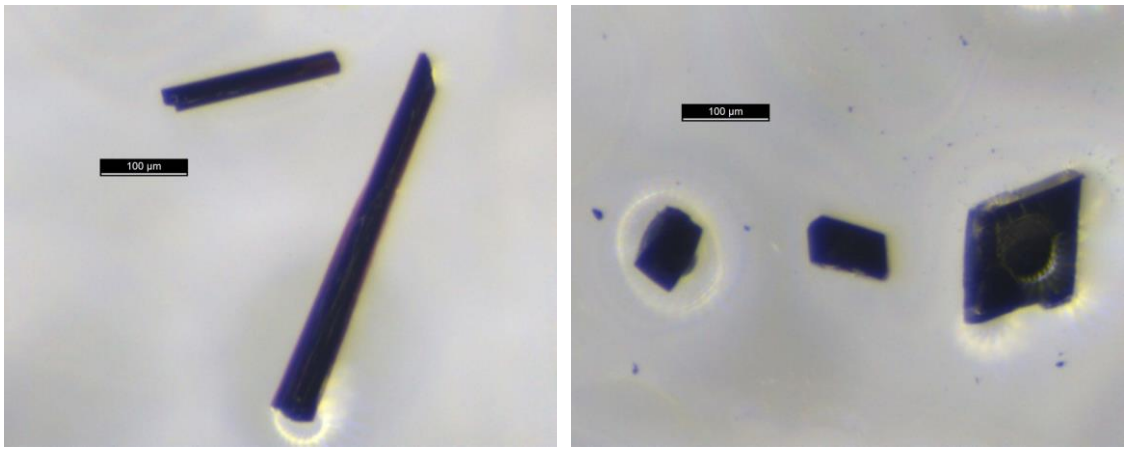


**Figure S8.** Picture of $(TMTSF)_2(TaF_6)_{0.84}(PF_6)_{0.16}$ needles (left) and picture of $(TMTSF)_3Ta_2F_{10}O$ prisms.

## $^{19}$F NMR spectroscopy of TMTSF salts

Nuclear magnetic resonance spectra were recorded on a Bruker Avance DRX 500 spectrometer operating at 470 MHz for 19F. Chemical shifts are expressed in parts per million (ppm). The following abbreviations are used: b, broad; s, singlet; d, doublet; quint, quintet; m, multiplet.

$(TMTSF)_2(TaF_6)_{0.12}(PF_6)_{0.88}$

*$^{19}$F NMR (DMSO-d6, 500 MHz, δ in ppm): -70.90/-69.39 (d, J = 755 Hz) for P**F**$_6^-$ / -4.92, 18.34 (d), 33.68 (d, $Ta_2F_{10}O$, $8F_{eq}$) and 41.48 (bs, $TaF_6$) for Ta**F**$_6^-$ and $Ta_2$**F**$_{10}$O. The integration gives ≈ 68% $PF_6^-$.*

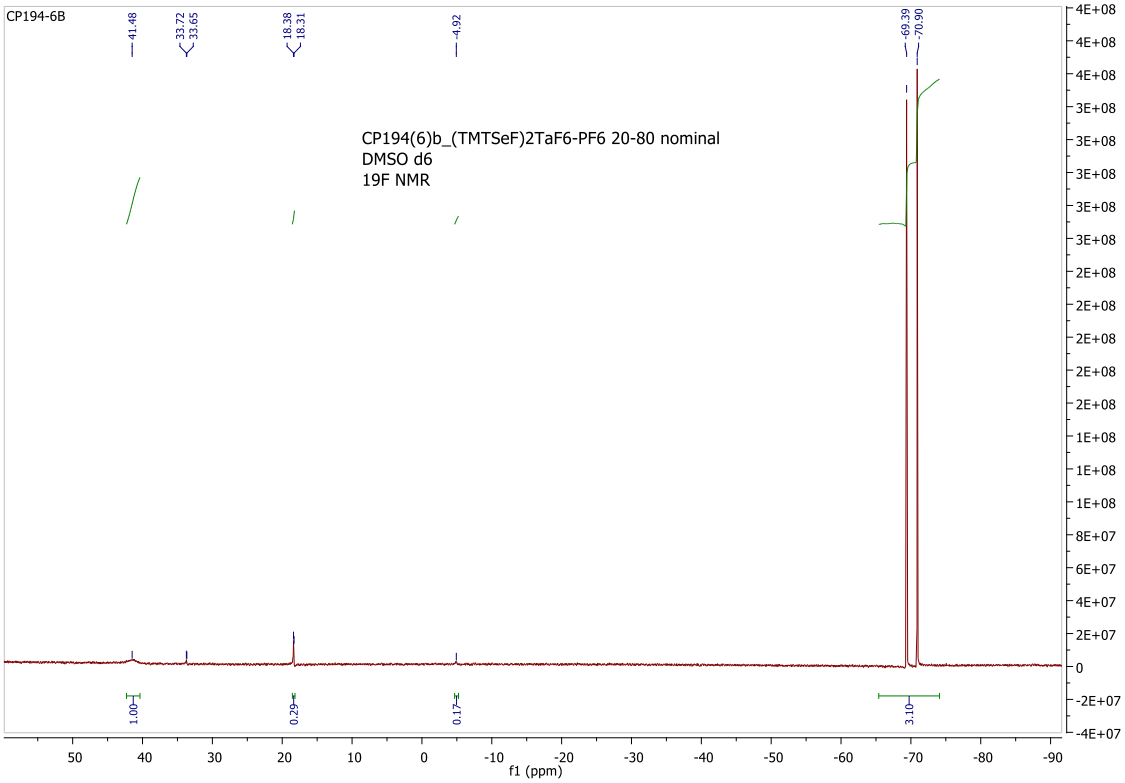


**Figure S9.** $^{19}$F NMR (DMSO-d6) spectrum of the crystalline material obtained by electrocrystallization of TMTSF with a mixture ($n$-$Bu_4N$)$TaF_6$ / ($n$-$Bu_4N$)$PF_6$ of nominal composition Ta/P 0.2/0.8.

$(TMTSF)_2(TaF_6)_{0.44}(PF_6)_{0.56}$

*$^{19}F$ NMR (DMSO-d6, 500 MHz, δ in ppm): -70.90/-69.39 (d, J = 755 Hz) for P**F**$_6^-$ / -4.90 (quint), 18.35 (d) and 41.32 (bs, $TaF_6$) for Ta**F**$_6^-$ and $Ta_2$**F**$_{10}$O. Integration gives ≈ 52% of $PF_6^-$.*

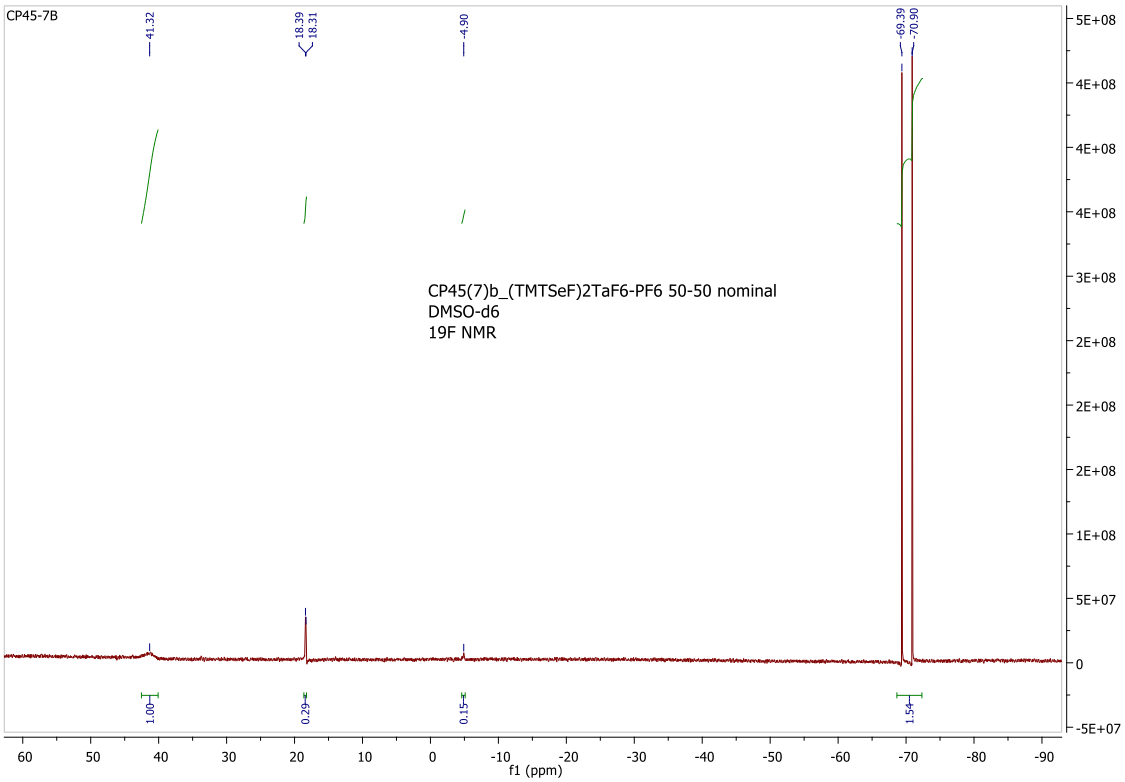


**Figure S10.** $^{19}F$ NMR (DMSO-d6) spectrum of the crystalline material obtained by electrocrystallization of TMTSF with a mixture (*n*-$Bu_4N$)$TaF_6$ / (*n*-$Bu_4N$)$PF_6$ of nominal composition Ta/P 0.5/0.5.

$(TMTSF)_2(TaF_6)_{0.56}(PF_6)_{0.44}$

*$^{19}F$ NMR (DMSO-d6, 500 MHz, δ in ppm): -70.90/-69.38 (d, J = 760 Hz) for P**F**$_6^-$ / -5.01 (quint), 18.32 (d) and 41.12 (bs, $TaF_6$) for Ta**F**$_6^-$ and $Ta_2$**F**$_{10}$O. Integration gives ≈ 60% of $PF_6^-$.*

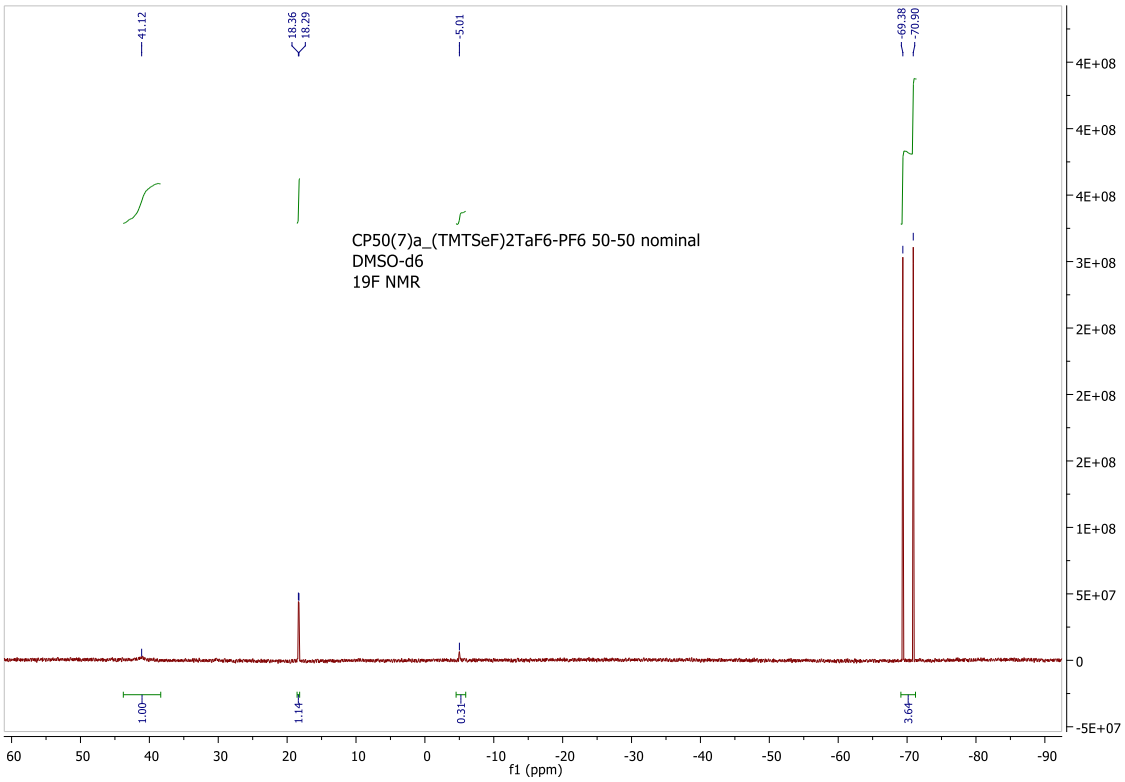


**Figure S11.** $^{19}F$ NMR (DMSO-d6) spectrum of the crystalline material obtained by electrocrystallization of TMTSF with a mixture ($n$-$Bu_4N$)$TaF_6$ / ($n$-$Bu_4N$)$PF_6$ of nominal composition Ta/P 0.5/0.5.

$(TMTSF)_2(TaF_6)_{0.84}(PF_6)_{0.16}$

*$^{19}F$ NMR (DMSO-d6, 500 MHz, δ in ppm): -70.90/ -69.39 (d, J = 755 Hz) for P**F**$_6^-$ / -5.26 (quint), 18.28 (d), 33.73 (d, $Ta_2F_{10}O$, $8F_{eq}$) and 41.48 (bs, $TaF_6$) for Ta**F**$_6^-$ and $Ta_2$**F**$_{10}$O. Integration gives ≈ 16% of $PF_6^-$.*

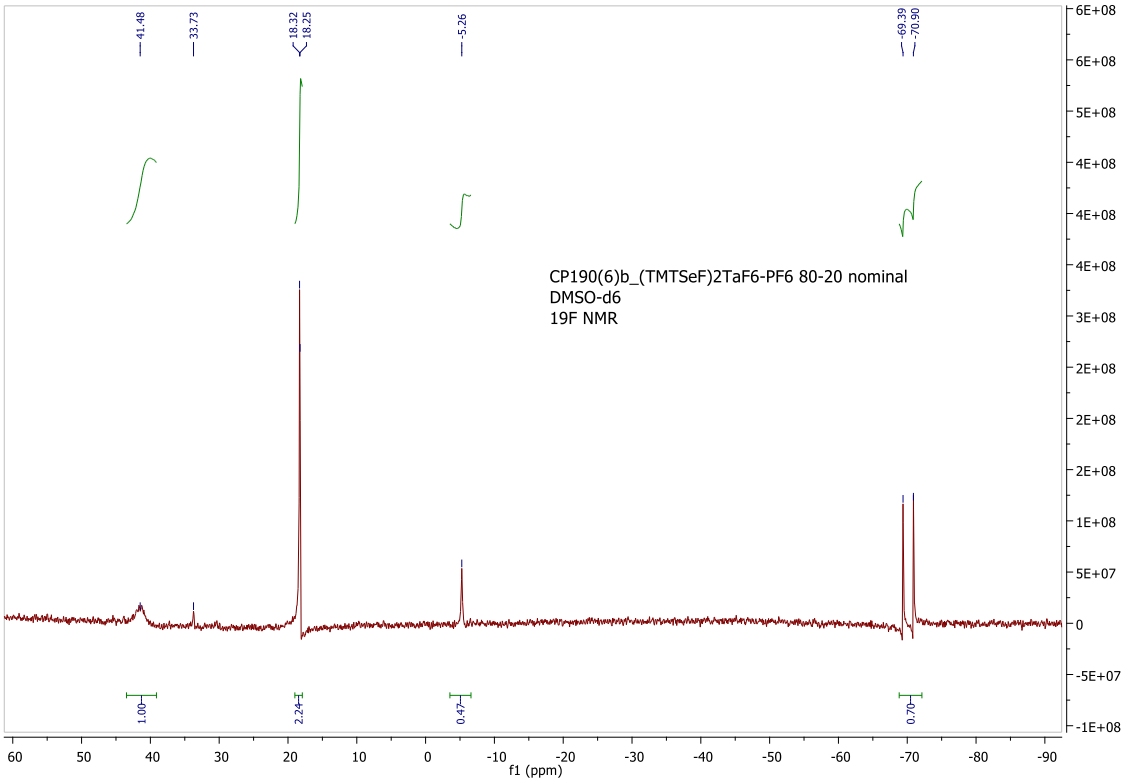


**Figure S12.** $^{19}F$ NMR (DMSO-d6) spectrum of the crystalline material obtained by electrocrystallization of TMTSF with a mixture ($n$-$Bu_4N$)$TaF_6$ / ($n$-$Bu_4N$)$PF_6$ of nominal composition Ta/P 0.8/0.2.

## Crystal structures of BEDT-TTF salts

Compound $\delta_o$-(BEDT-TTF)$_2$(TaF$_6$)$_{0.43}$(PF$_6$)$_{0.57}$

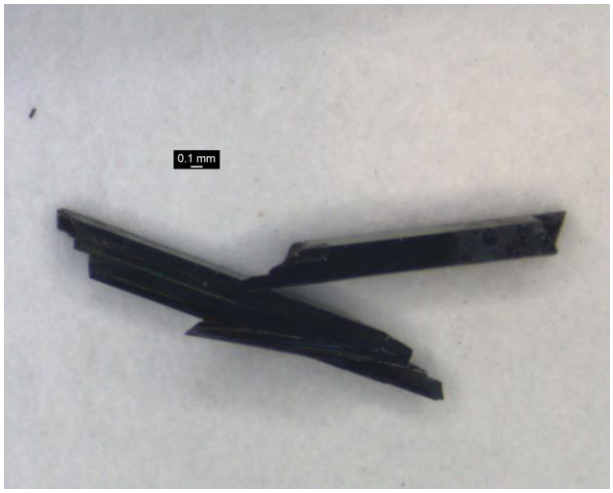


**Figure S13.** Picture of $\delta_o$-(BEDT-TTF)$_2$(TaF$_6$)$_{0.43}$(PF$_6$)$_{0.57}$ needles.

Compound $\delta_m$-(BEDT-TTF)$_2$(TaF$_6$)$_{0.94}$(PF$_6$)$_{0.06}$

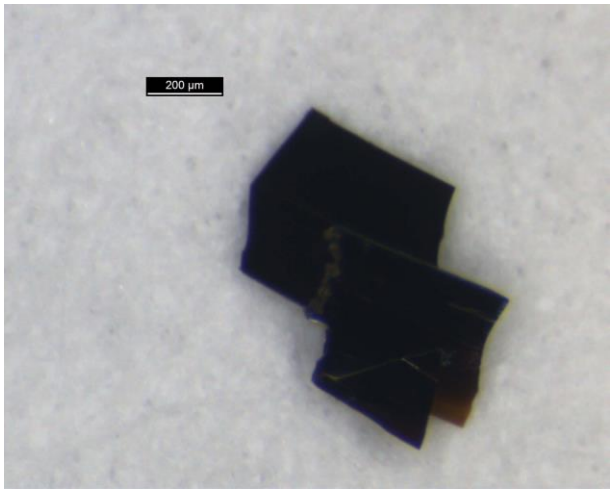


**Figure S14.** Picture of $\delta_m$-(BEDT-TTF)$_2$(TaF$_6$)$_{0.94}$(PF$_6$)$_{0.06}$ platelets.

## $^{19}$F NMR spectroscopy

The crystalline material was dissolved in DMSO-d6.

*$^{19}$F NMR (DMSO-d6, 500 MHz, δ in ppm): -70.90/-69.39 (d, J = 755Hz) for P**F**$_6$ / 18.32 (d), 33.66 (d, $Ta_2F_{10}O$, $8F_{eq}$) and 41.39 (m) for Ta**F**$_6$. Integration gives ≈ 6% of $PF_6$.*

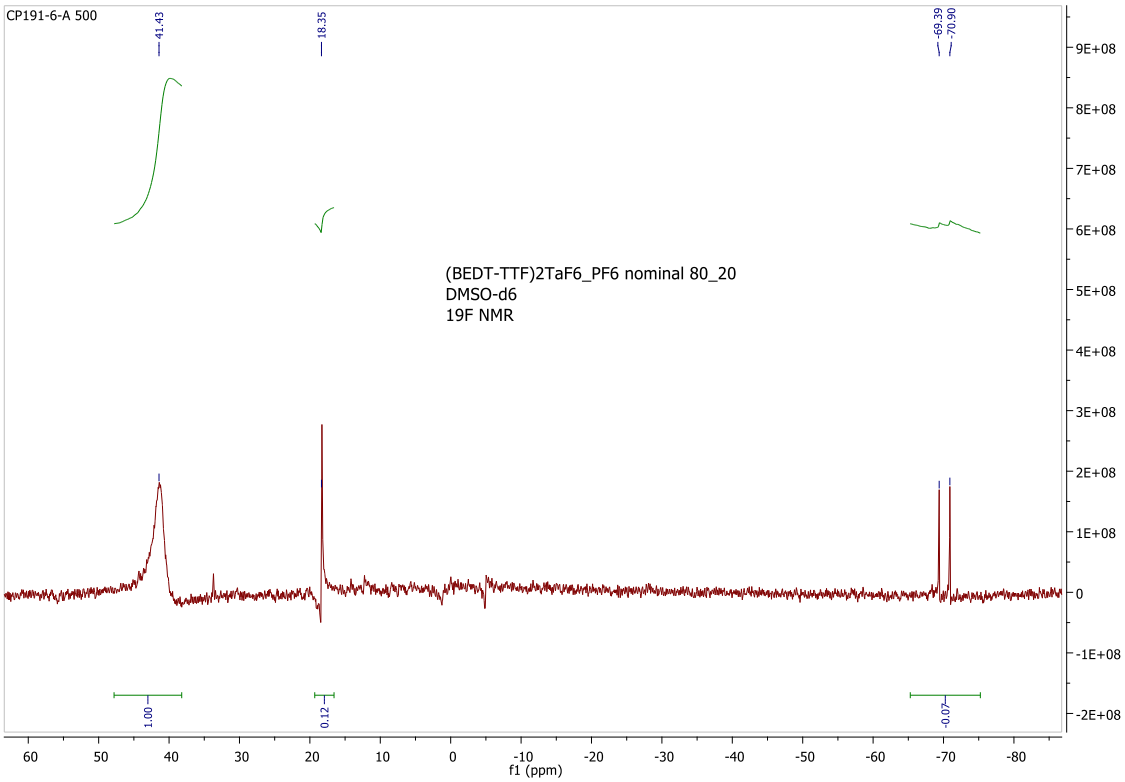


**Figure S15.** $^{19}$F NMR (DMSO-d6) spectrum of the crystalline material obtained by electrocrystallization of BEDT-TTF with a mixture (*n*-$Bu_4N$)$TaF_6$ / (*n*-$Bu_4N$)$PF_6$ of nominal composition Ta/P 0.8/0.2.

Compound $(BEDT\text{-}TTF)_2(TaF_6)_2{\cdot}CH_2Cl_2$

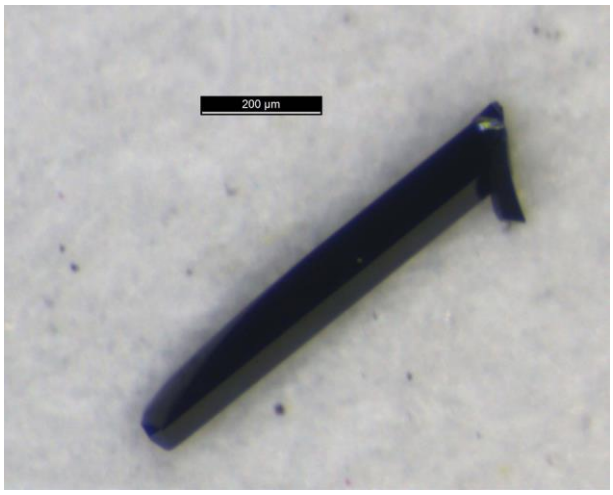


**Figure S16.** Picture of $(BEDT\text{-}TTF)_2(TaF_6)_2{\cdot}CH_2Cl_2$ thick needles.

**Table S3**. Comparison of the proportion of phosphorus and tantalum between the inserted precursor salts used for the electrocrystallization syntheses (nominal ratio), the refined ratio in the corresponding crystallographic structures (refined ratio) and the $^{19}F$ NMR integration in the TMTSF and BEDT-TTF salts.

| **Donor** | **TMTSF** | **TMTSF** | **TMTSF** | **TMTSF** | **BEDT-TTF** | **BEDT-TTF** |
|---|---|---|---|---|---|---|
| **Nominal rate** | 20%-(*n*-$Bu_4N$)$TaF_6$<br>80%-(*n*-$Bu_4N$)$PF_6$ | 50%-(*n*-$Bu_4N$)$TaF_6$<br>50%-(*n*-$Bu_4N$)$PF_6$ | 50%-(*n*-$Bu_4N$)$TaF_6$<br>50%-(*n*-$Bu_4N$)$PF_6$ | 80%-(*n*-$Bu_4N$)$TaF_6$<br>20%-(*n*-$Bu_4N$)$PF_6$ | 20%-(*n*-$Bu_4N$)$TaF_6$<br>80%-(*n*-$Bu_4N$)$PF_6$ | 80%-(*n*-$Bu_4N$)$TaF_6$<br>20%-(*n*-$Bu_4N$)$PF_6$ |
| **Crystal refined rate** | Ta: 0.12<br>P: 0.88 | Ta: 0.44<br>P: 0.56 | Ta: 0.56<br>P: 0.44 | Ta: 0.84<br>P: 0.16 | Ta: 0.43<br>P: 0.57 | Ta: 0.94<br>P: 0.06 |
| **Crystal Formula** | $(TMTSF)_2$<br>$(TaF_6)_{0.12}(PF_6)_{0.88}$ | $(TMTSF)_2$<br>$(TaF_6)_{0.44}(PF_6)_{0.56}$ | $(TMTSF)_2$<br>$(TaF_6)_{0.56}(PF_6)_{0.44}$ | $(TMTSF)_2$<br>$(TaF_6)_{0.84}(PF_6)_{0.16}$ | $\delta_o$-$(BEDT\text{-}TTF)_2$<br>$(TaF_6)_{0.43}(PF_6)_{0.57}$ | $\delta_m$-$(BEDT\text{-}TTF)_2$<br>$(TaF_6)_{0.94}(PF_6)_{0.06}$ |
| **$^{19}F$ NMR analysis** | Ta: 0.32<br>P: 0.68 | Ta: 0.48<br>P: 0.52 | Ta: 0.40<br>P: 0.60 | Ta: 0.84<br>P: 0.16 | - | Ta: 0.94<br>P: 0.06 |

**Table S4**. Central C=C and C–S internal bond distances (Å) of $(TMTSF)_2(TaF_6)_{0.12}(PF_6)_{0.88}$, $(TMTSF)_2(TaF_6)_{0.44}(PF_6)_{0.56}$, $(TMTSF)_2(TaF_6)_{0.56}(PF_6)_{0.44}$, $(TMTSF)_2(TaF_6)_{0.84}(PF_6)_{0.16}$ and $(TMTSF)_2TaF_6$ (293 K and 100 K).

| | **$(TMTSF)_2$ $(TaF_6)_{0.12}(PF_6)_{0.88}$** | **$(TMTSF)_2$ $(TaF_6)_{0.44}(PF_6)_{0.56}$** | **$(TMTSF)_2$ $(TaF_6)_{0.56}(PF_6)_{0.44}$** | **$(TMTSF)_2$ $(TaF_6)_{0.84}(PF_6)_{0.16}$** | **$(TMTSF)_2TaF_6$ (293 K)** | **$(TMTSF)_2TaF_6$ (100 K)** |
|---|---|---|---|---|---|---|
| **C1—C2** | 1.355(8) | 1.355(4) | 1.359(9) | 1.347(9) | 1.356(12) | 1.352(7) |
| **Se1—C1** | 1.861(6) | 1.876(3) | 1.874(6) | 1.874(5) | 1.875(8) | 1.882(5) |
| **Se2—C1** | 1.879(7) | 1.877(3) | 1.874(5) | 1.889(6) | 1.886(8) | 1.884(5) |
| **Se3—C2** | 1.884(6) | 1.881(3) | 1.876 (5) | 1.884(6) | 1.878(8) | 1.878(5) |
| **Se4—C2** | 1.885(6) | 1.877(3) | 1.881(5) | 1.876(5) | 1.875(8) | 1.880(5) |

**Table S5**. Central C=C and C–S internal bond distances (Å) of $\delta_o$-$(BEDT\text{-}TTF)_2(TaF_6)_{0.43}(PF_6)_{0.57}$, $\delta_m$-$(BEDT\text{-}TTF)_2(TaF_6)_{0.94}(PF_6)_{0.06}$ and $(BEDT\text{-}TTF)_2(TaF_6)_2{\cdot}CH_2Cl_2$.

| | **$\delta_o$-$(BEDT\text{-}TTF)_2$ $(TaF_6)_{0.43}(PF_6)_{0.57}$** | **$\delta_m$-$(BEDT\text{-}TTF)_2$ $(TaF_6)_{0.94}(PF_6)_{0.06}$** | **$(BEDT\text{-}TTF)_2$ $(TaF_6)_2$, $CH_2Cl_2$** |
|---|---|---|---|
| **C1—C2** | 1.362(4) | 1.356(7) | 1.386(5) |
| **S1—C1** | 1.732(3) | 1.735(5) | 1.721(4) |
| **S2—C1** | 1.737(3) | 1.745(6) | 1.716(4) |
| **S3—C2** | 1.738(3) | 1.739(5) | 1.721(4) |
| **S4—C2** | 1.738(3) | 1.737(5) | 1.720(4) |

**Single crystal resistivity measurements**

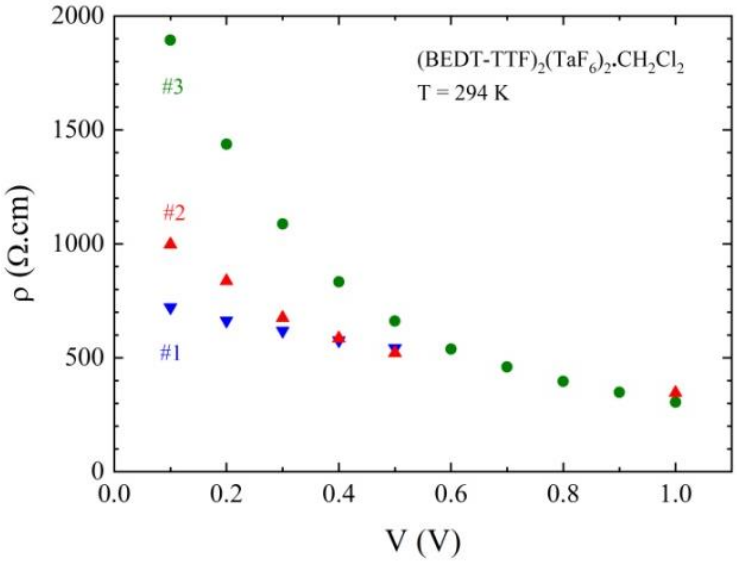


**Figure S17**. Electrical resistivity of three single crystals of $(BEDT\text{-}TTF)_2(TaF_6)_2{\cdot}CH_2Cl_2$ at room temperature plotted as a function of the applied voltage used for a two contact measurement.

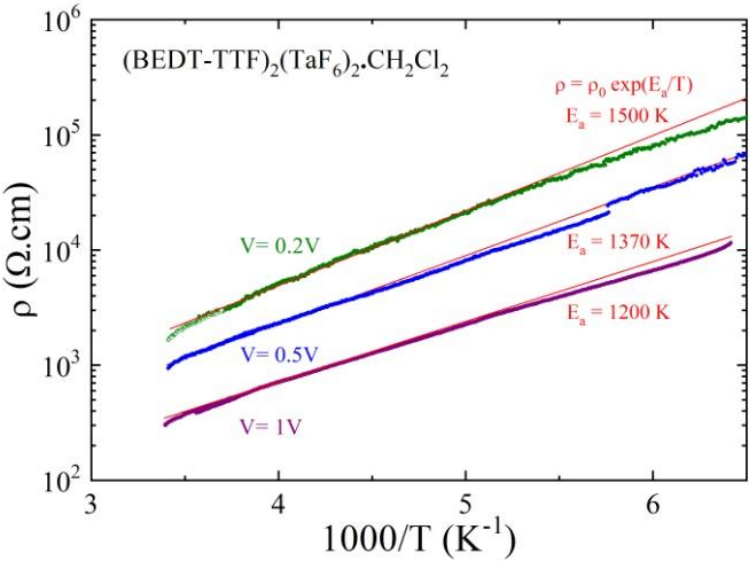


**Figure S18**. Temperature dependence of the electrical resistivity of a single crystal (#3) of $(BEDT\text{-}TTF)_2(TaF_6)_2{\cdot}CH_2Cl_2$ plotted as log ρ versus 1/T measured with different applied voltages: 0.2, 0.5 and 1 V. The red line is the linear fit to the data giving the activation energy $E_a$.